Low-loss singlemode large mode area all-silica photonic bandgap fiber

S. Février, R. Jamier and J.-M. Blondy

XLIM – IRCOM, UMR CNRS n°6172
Université de Limoges, 123 Avenue A. Thomas, 87060 Limoges – France
fevrier@xlim.fr

S. L. Semjonov, M. E. Likhachev, M. M. Bubnov and E. M. Dianov

Fiber Optics Research Center at GPI,
38 Vavilov Street, Moscow, 119991, Russia
sls@fo.gpi.ru

V. F. Khopin, M. Y. Salganskii and A. N. Guryanov

Institute of Chemistry of High Purity Substances,
49 Tropinin Street, Nizhny Novgorod, 603950, Russia
tvs@ihps.nnov.ru

Abstract: We describe the design and characterization of solid core large mode area bandgap fibers exhibiting low propagation loss and low bend loss. The fibers have been prepared by modified chemical vapor deposition process. The bandgap guidance obtained thanks to a 3-bilayer periodic cladding is assisted by a very slight index step (5.10^{-4}) in the solid core. The propagation loss reaches a few dB/km and is found to be close to material loss.

OCIS codes: (060.2280) Fiber design and fabrication; (060.2270) Fiber characterization.

References and links

1. K. P. Hansen, J. Broeng, P. M. W. Skovgaard, J. R. Folkenberg, M. D. Nielsen, A. Petersson, T. P. Hansen, C. Jakobsen, H. R. Simonsen, J. Limpert, F. Salin, "High-power photonic crystal fiber lasers: Design, handling and subassemblies," presented at Photonics West, San Jose, CA, (2005)
2. J. C. Knight, T. A. Birks, P. St. J. Russell, D. M. Atkin, "All-silica single-mode optical fiber with photonic crystal cladding," Opt. Lett. **21**, 1547-1549 (1996)
3. J. Limpert, A. Liem, M. Reich, T. Schreiber, S. Nolte, H. Zellmer, A. Tünnermann, J. Broeng, A. Petersson, C. Jakobsen, "Low-nonlinearity single-transverse-mode ytterbium-doped photonic crystal fiber amplifier," Opt. Express **12**, 1313-1319 (2004).
4. W. S. Wong, W. Peng, J. M. McLaughlin, L. Dong, "Robust single-mode propagation in optical fibers with record effective areas," presented at CLEO US, post deadline paper CPDB10, (2005)
5. S. Février, P. Viale, F. Gerome, P. Leproux, P. Roy, J.-M. Blondy, B. Dussardier, G. Monnom, "Very large effective area singlemode photonic bandgap fiber," Electron. Lett. **39**, 1240-1242 (2003)
6. A. Argyros, T. A Birks, S. G. Leon-Saval, C.M. B. Cordeiro, F. Luan, P. St. J. Russell, "Photonic bandgap with an index step of one percent," Opt. Express **13**, 309-314 (2005),
7. G. Bouwmans, L. Bigot, Y. Quiquempois, F. Lopez, L. Provino, and M. Douay, "Fabrication and characterization of an all-solid 2D photonic bandgap fiber with a low-loss region (< 20 dB/km) around 1550 nm," Opt. Express **13**, 8452 – 8459 (2005).
8. Jeunhomme, L.B., "Attenuation" in *Single-mode fiber optics*, eds. (Dekker, New York, 1990), pp. 96-101
9. M.A. Duguay, Y.Kokubun, T.L. Koch, L. Pfeiffer, "Antiresonant reflecting optical waveguides in SiO_2-Si multilayer structures," Appl. Phys. Lett. **49,** 13-15 (1986).
10. Litchinitser, S. C.Dunn, B. Usner, B.J. Eggleton, T.P. White, R. C. McPhedran, C. Martjin de Sterke, "Resonances in microstructured optical waveguides," Opt. Express **11**, 1243-1251 (2003).
11. J. Marcou, S. Février, "Comments on "On the analysis of a weakly guiding doubly clad dielectric optical fiber with an annular core," Microwave Opt. Technol. Lett. **38,** 248-254 (2003).

#9566 - $15.00 USD Received 17 November 2005; revised 9 January 2006; accepted 9 January 2006

12. S.G. Johnson, M. Ibanescu, M. Skorobogatiy, O. Weisberg, T.D. Engeness, M. Soljacic, S.A. Jacobs, J.D. Joannopoulos, Y. Fink, "Low-loss asymptotically single-mode propagation in large-core Omniguide fibers," Opt. Express **9**, 748-779 (2001)
13. S. Février, P. Roy, D. Pagnoux, J.-L. Auguste, J.-M. Blondy, J. Marcou, "12nm FWHM 20dB stop-band filter based on cascaded dual concentric core fiber filters," Electron. Lett. **37**, 1113-1114 (2001)
14. S. Février, J.-L. Auguste, J.-M. Blondy, J. Marcou, A. Peyrilloux, P. Roy, D. Pagnoux, "Accurate tuning of the highly-negative-chromatic-dispersion wavelength into a dual concentric core fibre by macro-bending," presented at 28th European Conference on Optical Communication, Copenhagen, Denmark, 8-12 september 2002
15. G. Humbert, F. Benabid, J. C. Knight, P. St. J. Russell, "Nonlinear effects due to interface modes in a hollow core photonic crystal fiber," presented at CLEO US, paper CMD5 (2005)
16. S. Février, R. Jamier, J.-M. Blondy, S. L. Semjonov, M. E. Likhachev, M. M. Bubnov, E. M. Dianov, V. F. Khopin, M. Y. Salganskii, A. N. Guryanov, "Low Loss Large Mode Area Bragg Fibre," presented at 31th European Conference on Optical Communication, Post deadline paper Th4.4.3, Glasgow, United-Kingdom, 25-29 september 2005
17. M. D. Nielsen, N. A. Mortensen, M. Albertsen, J. R. Folkenberg, A. Bjarklev, D. Bonacinni, "Predicting macrobending loss for large-mode area photonic crystal fibers," Opt. Express **12**, 1775-1779 (2004),

1. Introduction

In high power fiber lasers, nonlinear effects severely alter the spatial and spectral beam qualities. To increase their threshold of appearance, Large Mode Area Fibers (LMAFs) are currently used. The increase in the core diameter has also the advantage to increase the doped area and thus the available output power. Step-index LMAFs are limited in the singlemode regime (necessary to reach diffraction-limited output beams) to core diameter $D \sim 25$ µm at $\lambda = 1.08$ µm corresponding to the emission wavelength of Yb^{3+}-doped fiber lasers [1]. In this case, curvature loss severely limits packaging and implies the use of almost straight fibers, making the laser somewhat cumbersome. Endlessly singlemode photonic crystal fibers (PCF) are also employed [2]. The core diameter can be increased to 40 µm at the cost of a slightly multimode propagation. High-order mode filtering obtained by appropriate curvature allows to reach singlemodedness and very good spatial beam quality ($M^2<1.1$) [3]. Simpler holey fiber consisting of a solid core surrounded by a single ring of large holes has also proved to be a good candidate [4].

Solid core photonic bandgap fibers such as Bragg fibers [5] or low-index step PCFs [6,7] can also be used. The first case is of particular interest since the whole preform is made by Modified Chemical Vapor Deposition (MCVD) process only. The proposed Bragg fiber [5] was composed of high- and low-index concentric layers surrounding a low index broad ($D \sim 34$ µm) core. The high-index layers were Ge-doped so as to reach an index difference $\Delta n = 5.10^{-3}$. A thin fluorine doped outer layer was added to decrease curvature loss. Singlemode operation in a 4-m-long sample was observed. Inaccuracy of the refractive index profile (RIP) together with the small index difference in the cladding layers have led to relatively high propagation loss (~1 dB/m).

Reducing the propagation loss is of primary interest since in future rare-earth-doped LMA Bragg fiber laser or amplifier applications background loss will severely limit the net gain. Moreover practical use of these fibers could greatly take advantage of lowered bend loss. In this paper we demonstrate an improved design of LMA bandgap fiber with low confinement loss and report on characterization of fabricated fibers. We show that LMA fiber with low bend-sensitivity can be realized with widespread MCVD technique.

2. Design considerations

An example of considered index profile is shown in Fig. 1(a). The fiber consists of a low-index core surrounded by high- and low-index layers with index contrast Δn. In bandgap fibers, confinement loss can be limited by increasing the number of cladding layers or increasing Δn. Confinement loss in large core ($D = 22 \lambda$) bandgap fiber has been computed

#9566 - $15.00 USD Received 17 November 2005; revised 9 January 2006; accepted 9 January 2006

versus wavelength and plotted in Fig. 1(b) for values of Δn achievable by MCVD. The maximum index contrast considered is 50.10^{-3}, implying validity of the weak guidance approximation. Thus computations were carried out using a standard one-dimensional solver for the scalar wave equation. Confinement loss was compared to material loss computed taking into account a pure-silica core [8].

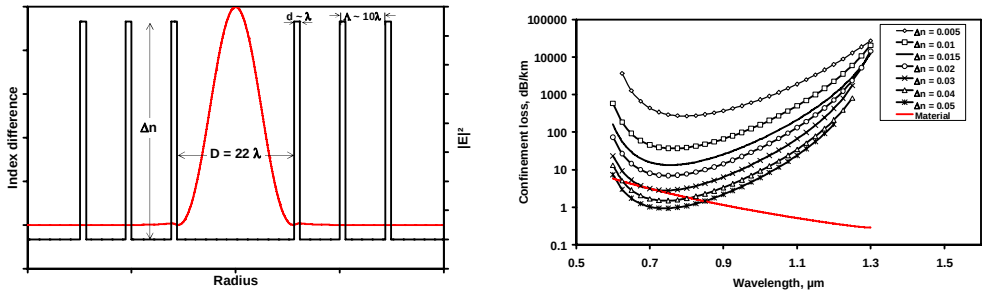

(a) (b)

Fig. 1. (a) Refractive index profile and electric field intensity distribution of considered bandgap fiber. The core, high-*n* layer and low-*n* layer thicknesses are 22 λ, λ, 9 λ, respectively. (b) Confinement loss computed versus the wavelength for different values of Δn. Also reported is the material loss.

Bragg fiber proposed is the low-Δn cylindrical version of antireflecting resonant optical waveguide (ARROW) proposed by Duguay *et al*. [9]. In such waveguides, provided the wavelength is much smaller than the cladding periodicity (See Fig. 1(a)), the spectral properties of the core mode can be deduced from the thickness (d) and Δn of the first high-index ring. Low-loss spectral ranges are separated by large attenuation peaks attributed to cut-off of the ring modes [10]. Due to the cylindrical symmetry of the proposed fiber only modes with zero azimuthal order have to be considered. Thus the band edges coincide with the cut-off wavelengths ($\lambda_c^{0,n}$) of the $LP_{0,n}$ modes of the ring where n > 0 is the radial order. $\lambda_c^{0,n}$ can be solved for using the dispersion relation of the annular waveguide [11]. For an ideal fiber with $\Delta n = 30.10^{-3}$ and d = 1.07 μm $\lambda_c^{01} \rightarrow \infty$, $\lambda_c^{02} = 0.606$ μm and $\lambda_c^{03} = 0.301$ μm. The band edge located at 0.6 μm is clearly seen in Fig. 1(b).

As demonstrated earlier [5], $\Delta n = 5.10^{-3}$ leads to propagation loss around 1 dB/m. Since the loss decreases when increasing Δn, a large index contrast (Δn > 0.03) is necessary to reach confinement loss lower than material loss (~2 dB/km at λ = 0.8 μm). A second improvement can be done by slightly raising the core index. An example of this improved design is shown in Fig. 2(a). Index difference in the core is Δn_{core}.

First the intensity distribution of the Bragg mode has been computed and plotted in Fig. 2(a). No major change has been brought compared to the distribution plotted in Fig. 1(a). Then the curve of effective index (n_e) of the Bragg mode has been plotted in Fig. 2(b) versus the wavelength and compared to pure-silica cladding index and doped ($\Delta n = 3.10^{-4}$) core index. It is worth to note that n_e is comprised between those two indices for λ < 0.85 μm indicating total-internal-reflection guidance mechanism occurs for this spectral range. By looking at the electric field distribution for λ = 0.8μm, magnified in Fig. 2(c) for the purpose of clarity, one can observe the canceling at the low-*n* to high-*n* transitions which is a feature of ARROWs [9]. Hence, the index-raised core implies a dual photonic bandgap and total internal reflection waveguidance mechanism to occur at short wavelengths. The confinement loss at λ = 0.8 μm has been computed and plotted in Fig. 2(d) for various Δn_{core}. Calculations show that an index step in the core as small as $\Delta n_{core} = 3.10^{-4}$ allows to decrease confinement loss around 0.01 dB/km.

#9566 - $15.00 USD Received 17 November 2005; revised 9 January 2006; accepted 9 January 2006

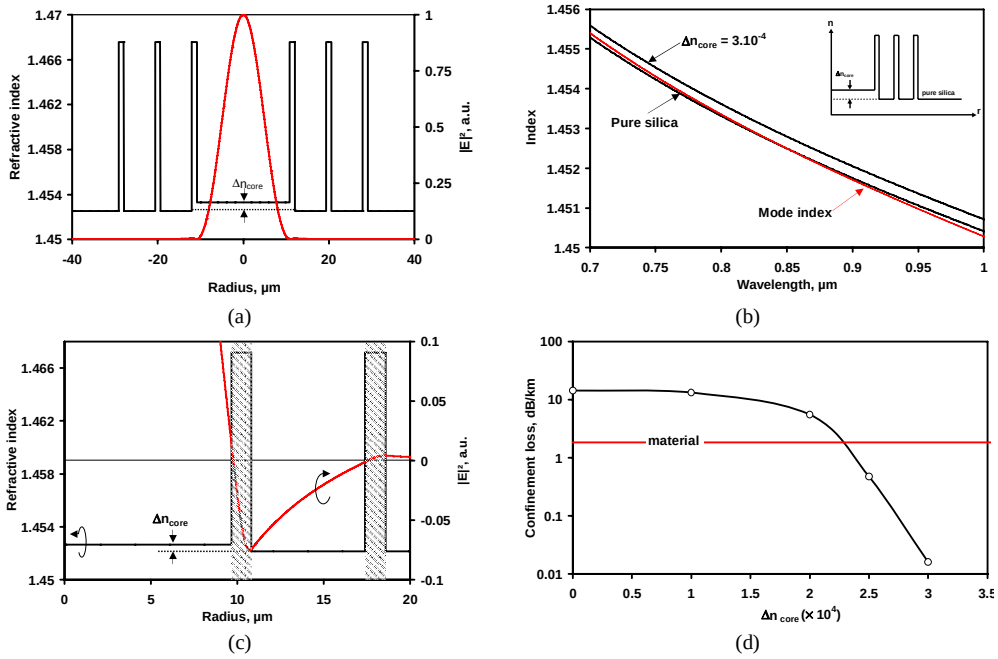

Fig. 2. (a) Refractive index profile and electric field intensity distribution of designed fiber. (b) Effective index n_e of the Bragg mode versus the wavelength compared to clad (pure-silica) index n_2 and core (raised) index $n_1 = n_2 + \Delta n_{core}$ showing $n_2 < n_e < n_1$ for $\lambda < 0.85$ µm, evidencing total-internal-reflection mechanism. (c) Radial electric field distribution canceling at low-n → high-n transitions and maximum at high-n → low-n transitions characteristic of the bandgap waveguidance mechanism. (d) Confinement loss computed at $\lambda = 0.8$ µm versus Δn_{core}. Δn in the cladding layers is 15.10^{-3}. Also reported is the material loss.

3. Fabrication

Accurately manufacturing such a positive index step is difficult by the MCVD process. On the other hand, the low-index layers may be F-doped so as to decrease the refractive index. Two preforms were prepared with $\Delta n = 15.10^{-3}$ and an effective $\Delta n_{core} = +5.10^{-4}$, values than can be readily obtained by MCVD process. The higher Δn_{core} was chosen to ensure lower confinement loss. The number of layers' pairs is still equal to 3. An outer F-doped layer was added to decrease bend loss.

Fibers were drawn with outer diameter (OD) equal to 125 µm, 170 µm and 220 µm so as to operate at 0.8 µm, 1.064 µm and 1.55 µm wavelengths, respectively. The measured RIP of the 125-µm-OD fibers are shown in Fig. 3.

In the very first manufactured fiber [5] the index transitions were very smooth. On the contrary in the new fiber the index transitions are steep. Moreover thicknesses fairly coincide with those deduced from the modeling stage. Note the RIPs are slightly different. In Fig. 3(b) the high-n layers are more Ge-doped. This should imply lower loss.

#9566 - $15.00 USD Received 17 November 2005; revised 9 January 2006; accepted 9 January 2006

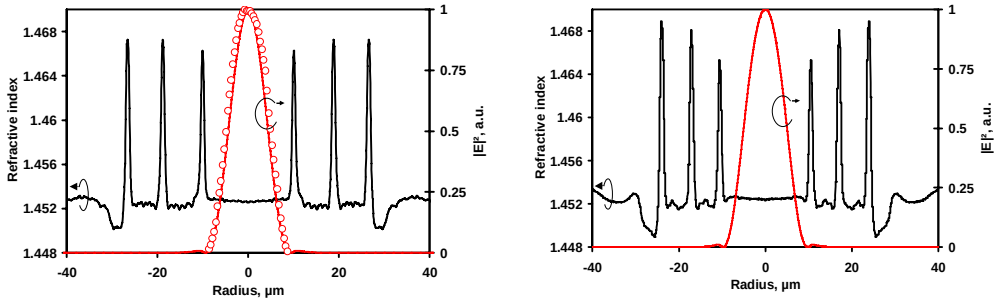

Fig. 3. Refractive index profile and electric field intensity distribution in two fabricated fibers (at $\lambda = 833$ nm). The fibers' outer diameter is 125 μm. Fibers were drawn from different preforms explaining the slightly different RIPs. Circles denote measured field intensity distribution while bold line denotes the field distribution computed taking into account the actual index profile.

4. Characterization

4.1 Singlemodedness

First, the modal behavior has been studied in the proposed structure. To do so, the beam from a singlemode fiber at short wavelengths (cut-off wavelength $\lambda_c = 0.77$ μm) has been travelled in front of the 125-μm-OD fiber along two orthogonal directions. This experiment was carried out for 2 pieces of fiber with lengths $L_1 = 1.2$ m and $L_2 = 30$ m drawn from the same preform. Near field intensity patterns have been plotted in Fig. 4 for centered and shifted excitations.

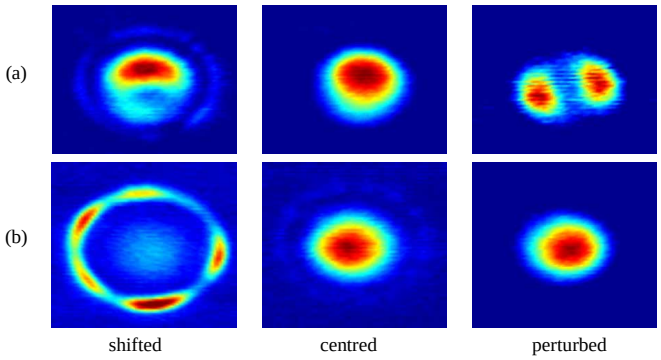

Fig. 4. Observed near field intensity patterns for (a) L = 1.2 m and (b) L = 30 m and for various launching conditions.

It is worth to note that the near field patterns of the short piece of fiber, obtained with shifted excitation, exhibit non Gaussian shape. This indicates a multimode behavior. On the other hand, whatever the launching conditions into the longest sample, the pattern in the core remains circular, indicating the 30-m-long fiber is singlemode. Obviously, when launching is strongly shifted, modes of the first high-index ring are excited. When propagation is perturbed (e.g. the fiber is bent with 2-cm curvature radius), the $LP_{1,1}$ mode is clearly observed in the short sample whereas the field pattern at the output of the longest sample remains circular. This experiment confirms the singlemode behavior of the 30-m-long piece of LMA bandgap fiber. Higher-order mode filtering through large loss discrimination is a feature of leaky waveguides such as bandgap fibers and makes possible the fabrication of very large mode area bandgap waveguides as anticipated by Duguay *et al.* [9]. Here, this results in vanishing of $LP_{1,1}$ mode after a sufficient propagation length. This behavior was referred to as asymptotically single-mode propagation by Johnson *et al.* [12]. Experimental and computed

#9566 - $15.00 USD Received 17 November 2005; revised 9 January 2006; accepted 9 January 2006

radial intensity distributions are shown in Fig. 3(a) and found in excellent agreement. The effective area of the fundamental mode has been computed to 140 µm² at 833 nm.

This operation has been made for the various fiber samples and the same conclusions were drawn. The fibers are asymptotically singlemode at their operating wavelengths.

4.2 Spectral attenuation

The attenuation spectrum of the 30-m-long piece of 125-µm-OD fiber has been measured by the cut-back technique and plotted in Fig. 5(a).

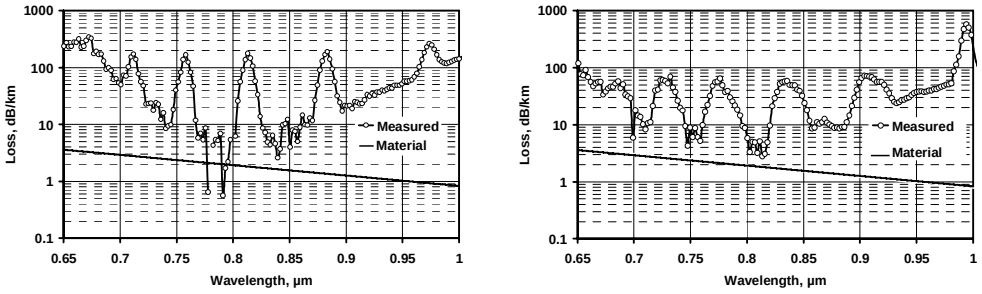

Fig. 5. Attenuation spectra for (a) L = 30 m, (b) L = 100 m. Also reported is the material loss. Differences in position and level of attenuation peaks arise from different RIPs.

The material loss spectrum is also reported. Broadband transmission has been observed from 0.7 µm to 1 µm. The minimal loss (~ 3 dB/km) occurs at a wavelength of 0.79 µm. The uncertainty on the measured value arises from the short length used. The loss spectrum of a 125-µm-OD fiber drawn from the other preform has been accurately measured using a 100-m-long sample. Results have been plotted in Fig. 5(b). The minimal attenuation reaches 2.8 dB/km at 0.81 µm. This value is very close to the material loss (2 dB/km). In these original structures, the confinement loss has been reduced to ~1 dB/km.

In the 170-µm-OD (resp. 220-µm-OD) sample, the minimal attenuation and the mode area have been measured around 10 dB/km (resp. 9 dB/km) and 270 µm² (resp. 500 µm²) at 1 µm (resp. 1.5 µm), respectively.

For all the fabricated fibers, multiple bands of very high (~100 dB/km) attenuation appear in the spectrum. To better understand this phenomenon, the near field intensity pattern has been observed in a large attenuation peak (See Fig. 5(a)) for the 125-µm-OD fiber. The Gaussian mode is coupled to the $LP_{8,1}$ mode of the annular waveguide consisting of the first high-index ring surrounded by the core and the first low-index ring. This F-doped layer is of finite dimension and the outer pure silica cladding was also considered. Extension of this layer is supposed to be infinite. Such discrete couplings have already been observed in dual concentric core fibers and used to realize spectral filters [13]. In the proposed fiber, the modes' parities differ and coupling should not occur. Let us point out the slight distortion of the $LP_{8,1}$ mode intensity distribution. The localization of the field in the first quadrant may be attributed to bending during the experiment [14]. Hence the overlap between the Bragg mode and the odd mode of the ring is not zero and coupling occurs. Such couplings are also a feature of hollow-core photonic crystal fibers, in which they allow for an exacerbation of nonlinear effects in silica [15]. We have then computed the effective index curves of the Bragg mode and of some of the high-order modes of the annular guide alone versus the wavelength (See Fig. 6(b)). These curves cross at specified phase-matching wavelengths. Thanks to longitudinal fluctuations of the RIP or bending, the modes couple around the phase-matching wavelengths.

#9566 - $15.00 USD Received 17 November 2005; revised 9 January 2006; accepted 9 January 2006

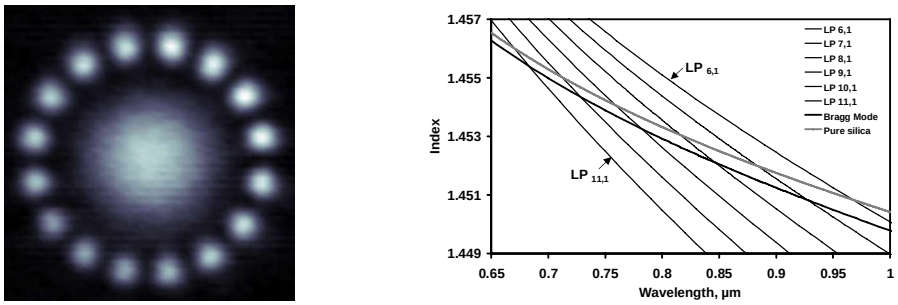

(a) (b)

Fig. 6. (a) Observed near field intensity pattern corresponding to the coupling between the Gaussian mode and the $LP_{8,1}$ mode of the first annular waveguide. (b) Effective index versus the wavelength for the Gaussian mode and some modes of the first annular waveguide. Also reported is the refractive index of pure silica.

One other important fact, pointed out in Fig. 6(b), is that the effective index of the Gaussian mode is smaller than the index of silica constituting the outer cladding whatever the wavelength is. Then the ring modes and the supermodes radiate outside the fiber (they are cut-off) and lead to large attenuation peaks. As shown in Table 1 the peak attenuation wavelengths correspond to the computed cut-off wavelengths and not to the phase-matching wavelengths.

Table 1. Comparison between peak attenuation wavelengths (λ_p), computed phase-matching wavelengths (λ_{pm}) and cut-off wavelengths (λ_c)

	$LP_{11,1}$	$LP_{10,1}$	$LP_{9,1}$	$LP_{8,1}$	$LP_{7,1}$
λ_p (nm)	674	712	758	813	884
λ_{pm} (nm)	682	730	780	848	924
λ_c (nm)	672	712	761	816	885

Cut-off is due to the F-doped inner cladding associated to the outer pure-silica cladding. To avoid these leaky couplings, an optimized fiber should not incorporate negative index step.

4.3 Bend loss

Bend loss has been measured in the 170-µm-outer diameter core fiber at a wavelength of 1.064 µm [16]. For the purposes of comparison, a singlemode step-index fiber has also been prepared by MCVD process. The cut-off wavelength of the SIF has been measured to 1003 nm. The mode field radius is 9.5 µm at 1.064 µm, equal to that of the bandgap fiber. Results have been plotted in Fig. 7. Refractive index profile of SIF is shown in in-set. The bandgap fiber appears to be less bend-sensitive than the step-index fiber. For instance, for a bend-radius equal to 8 cm, bend loss has been measured to 0.065 dB/m in the bandgap fibre and 1.16 dB/m in the SIF. The bend loss has also been computed in LMA photonic crystal fiber with hole-to-hole spacing $\Lambda = 15$ µm, hole diameter $d = 6.6$ µm ($d/\Lambda = 0.44$ for singlemode operation) and 8 rings of holes. The mode field radius is equal to 9.5 µm. Hence the PCF properties may be compared to those of bandgap and step-index fibers. Computations using the simple technique reported in [17] showed the PCF is less bend-sensitive than the SIF but more susceptible to curvature than the bandgap fiber.

#9566 - $15.00 USD Received 17 November 2005; revised 9 January 2006; accepted 9 January 2006

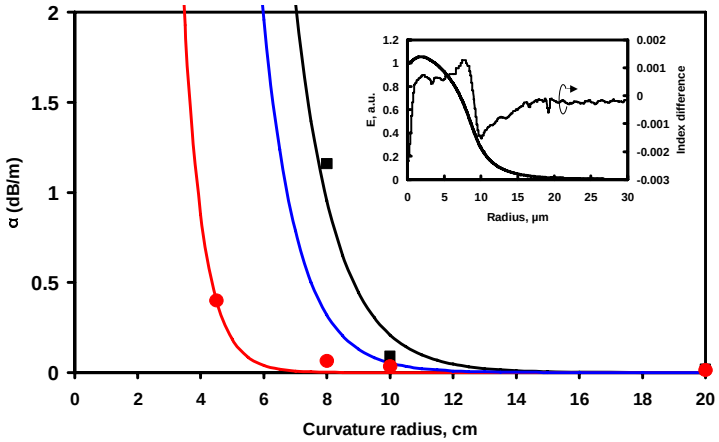

Fig. 7. Bend loss for bandgap fiber (red), step-index fiber (black) and ideal PCF (blue). Dots: measured data, lines: computed values. In-set: index profile and electric field distribution of SIF.

5. Conclusion

An improved fiber design associating total internal reflection and bandgap guidance mechanisms has been proposed to dramatically reduce confinement loss in large mode area fiber. Optimized fibers have been prepared by MCVD process. A loss reduction by 3 orders of magnitude has been demonstrated compared to the very first fabricated structure. No preconditioning is necessary to filter out high-order modes, provided the fiber is a few meter long. Couplings to cut-off modes of the first annular guide lead to high attenuation peaks. The minimal attenuation wavelength has been adjusted to 1.064 µm by properly scaling the fiber outer diameter. The bandgap fiber has been found to be much less bend-sensitive than step-index fibers with the same mode field diameter.

#9566 - $15.00 USD Received 17 November 2005; revised 9 January 2006; accepted 9 January 2006